

1 **Supporting Information for**

2 **Catalytic hydrogenation of CO₂ from air via porous silica-**
3 **supported Au nanoparticles in aqueous solution**

4 Siting Ni,^a Jun Zhu,^a Ranjan Roy,^b Chao-Jun Li^a and R. Bruce Lennox^{*a}

5 a. Department of Chemistry, McGill University, 801 Sherbrooke St. West, Montreal,
6 Quebec H3A 0B8, Canada

7 b. Department of Chemical Engineering, McGill University, M.H. Wong Building,
8 Montreal, Quebec H3A 0C5, Canada

9

11 **1. Materials and Methods**12 **2. Additional characterizations of Au/SiO₂**13 *Fig. S1.* EDS characterization of porous SiO₂ and Au/SiO₂.14 *Fig. S2.* UV-vis spectra of Au/SiO₂, porous SiO₂ and AuNPs.15 *Fig. S3.* XPS survey scan.16 *Fig. S4.* TEM images of DMAP-AuNPs.17 *Fig. S5.* Stability test of the Au/SiO₂.18 *Table S1.* Zeta potential of various samples.19 **3. The weight percentage of Au in the Au/SiO₂ composite**20 **4. Quantitative ¹³C NMR**21 *Fig. S6.* ¹³C NMR and T1 measurements.22 *Fig. S7.* NMR spectra of 3.2 wt. % PEHA CO₂ capture solution.23 *Fig. S8.* NMR spectra of 3.2 wt. % PEHA CO₂ capture solution after hydrogenation.24 **5. GC-TCD analysis of gas phase**25 *Table S2.* Retention time of various samples in GC-TCD26 *Fig. S9.* GC-TCD of the gas phase after a typical hydrogenation reaction.27 **6. Limit of Detection (LOD) and Limit of Analysis (LOA) Determination on GC-**
28 **TCD**29 *Table S3.* Limits of detection (LOD) and limits of analysis (LOA) (ml) of gas standard.30 *Fig. S10.* Certificate of the gas standard used in the calibration curves and the
31 determination of LOD and LOA.32 *Fig. S11.* Calibration curves.33 *Fig. S12.* Gas chromatograms of the gas standard with various injection volumes.34 *Fig. S13.* Gas chromatograms of the blank (no gas injection).35 **7. GC-MS identification and quantification of MeOH**

36 *Fig. S14.* GC-MS.

37 **8. Mechanistic studies:¹⁸O isotope study**

38 *Fig. S15.* Mass spectra.

39 *Fig. S16.* Calibration curve.

40 *Fig. S17.* Potential transformations in the isotope studies.

41 **9. Additional studies**

42 *Table S4.* Recently reported hydrogenation systems of amine-captured CO₂ to C1
43 products in (partially) aqueous similar to this work.

44 *Table S5.* Study of CO₂ hydrogenation in dilute PEHA solutions.

45 *Fig. S18.* Catalytic activities with different Au loadings.

46 *Fig. S19.* Product distribution and conversion with various reaction times.

47 **1. Materials and Methods**

48 Hexadecyltrimethylammonium bromide (CTAB, $\geq 99\%$), tetramethyl orthosilicate
49 (TMOS, 98%), 1,3,5-trimethylbenzene (TMB, 98%), pentaethylenehexamine (PEHA,
50 technical grade), and water- ^{18}O (97 atom % ^{18}O) were purchased from Sigma-Aldrich.
51 Methanol (ACS certified), anhydrous ethanol (ACS certified), and sodium hydroxide
52 (Pellet, ACS certified) were purchased from Fisher Scientific. Water used in preparation
53 procedures was obtained from a Milli-Q system (18 M Ω) except otherwise indicated. All
54 other chemicals were obtained from commercial suppliers and used without further
55 purification.

56 UV-Visible-NIR spectra were collected on an Agilent Technologies Cary 5000 UV-Vis-
57 NIR.

58 TEM images were obtained on a FEI Tecnai G2 F20 200 kV Cryo-STEM with a Gatan
59 Ultrascan 4000 4k x 4k CCD Camera System Model 895; EDS analysis was done by an
60 EDAX Octane T Ultra W /Apollo XLT2 SDD and TEAM EDS Analysis System built on
61 the STEM set up. TEM samples were prepared by drop-casting the solution on carbon-
62 coated copper TEM grids (CF-400-Cu, 25/pk, carbon film on 400 Square Mesh copper
63 grids, Electron Microscopy Science).

64 XPS spectra were recorded on a ThermoFisher Scientific K-alpha instrument equipped
65 with a monochromatic Al K α X-ray source (1486.6 eV). Survey scans and high-
66 resolution scans were collected on an X-ray spot size of 200 μm with energy steps of 1
67 and 0.1 eV, respectively. Spectral energies were calibrated by setting the C-C binding
68 energy of C1s at 284.8 eV. Peak fitting was performed using the Thermo Avantage
69 software (version 4.60). XPS samples were prepared by drop-casting a concentrated
70 solution on a copper foil and dried in a vacuum oven overnight.

71 BET measurements were made on a Micromeritics TriStar 3000 Surface Area and Pore
72 Size Analyzer. The analysis was performed by adsorption-desorption of nitrogen at
73 77.350 K.

74 Pressured reactions were carried out on a Biotage® Endeavor™ Catalyst Screening
75 System controlled by Endeavor® Advanced Software (EAS).

76 ^1H NMR and non-quantitative ^{13}C NMR spectra were recorded with Bruker AVIIIHD
77 500 MHz NMR Spectrometer in D_2O ; quantitative ^{13}C NMR spectra were recorded with
78 Bruker AVIIIHD 800 MHz NMR Spectrometer in D_2O .

79 GC-MS experiments were performed on an Agilent Technologies Gas Chromatograph
80 System equipped with a 5973 *Inert* Mass Selective Detector. The column Rtx-5 (30m,
81 0.25 mm ID, 0.25 μm df) from Restek Corporation was used.

82 GC-TCD experiments were performed on an Agilent Gas Chromatograph (GC) 6890
83 equipped with a Split/Splitless injector, an integrate valve switch and a thermal
84 conductivity detector (TCD) was used for the reactor gas analysis. The GC was
85 controlled by Chemstation Software. All injections were manual injections from a sealed
86 gas bag. The syringe system used was VICI Precision Lock Syringe from a volume of 10
87 μl to 2000 μl . Specifically:

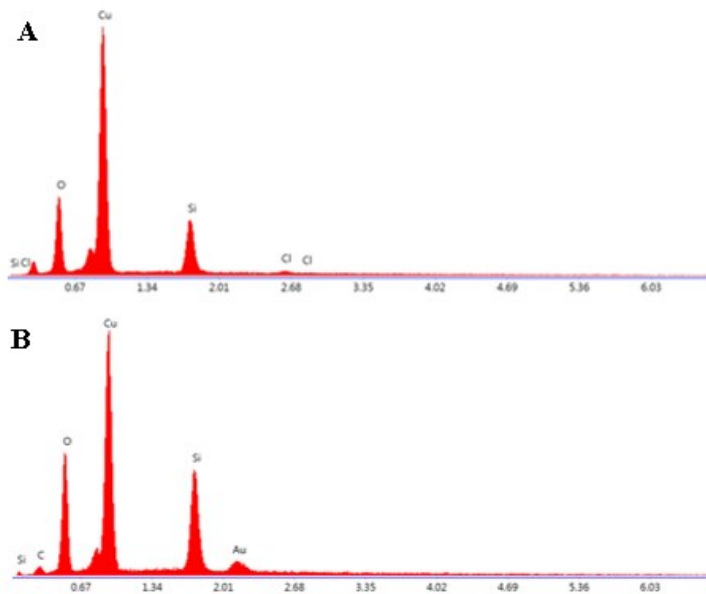
88 **Injector:** The injector was used in split mode with a 10:1 split ratio. It was maintained at
89 a constant 200 $^\circ\text{C}$ with a total flow of 163 ml/min. The carrier gas was argon (99.995%).
90 The head pressure was maintained at 6.67 psi.

91 **Oven:** The oven was initially maintained at 30 $^\circ\text{C}$ for 9 minutes. It was then ramped at 50
92 $^\circ\text{C}/\text{min}$ to 120 $^\circ\text{C}$ and then maintained there for 8 minutes. The total run time was 19
93 minutes.

94 **Column:** Column 1 is an Agilent HP PLOT-Q column (30 m x 0.530 mm, 25.00 micron);
95 Column 2 is an Agilent HP-PLOT MoleSieve (30 m x 0.530 mm, 20.00 micron).

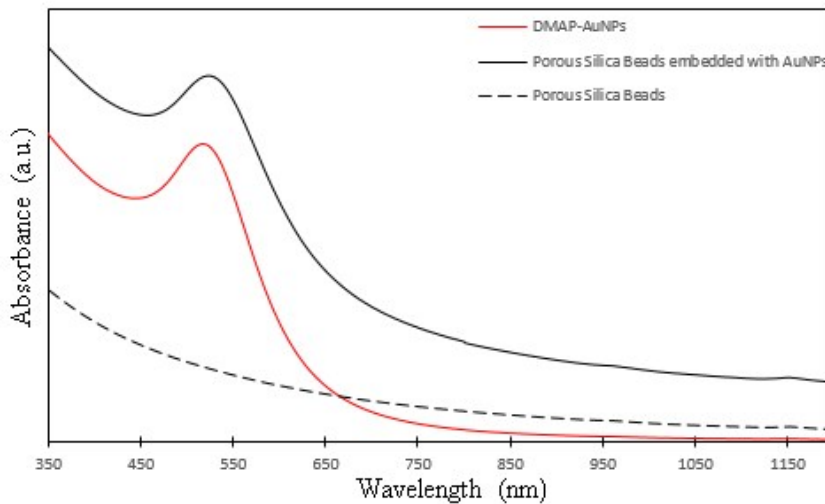
96 **Detector:** The TCD was maintained at 210 $^\circ\text{C}$ the reference flow was set at 30 ml/min
97 with Ar as the make-up gas at 0.6 ml/min. The filament was set to negative polarity.

98 **Switch Box:** The switch box was maintained at 100 $^\circ\text{C}$ with valve switches at 5.20
99 minutes and 11.00 minutes.



101 **2. Additional characterizations of Au/SiO₂**

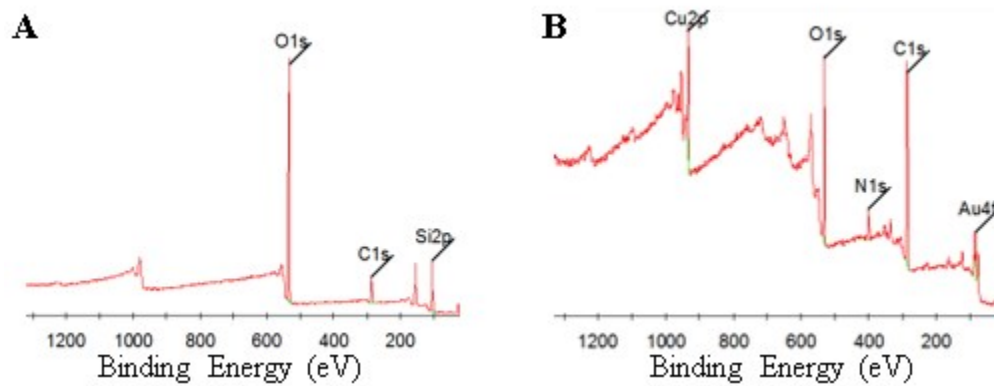
102 **Fig. S1.** EDS characterization of porous SiO₂ and Au/SiO₂. EDS analysis of porous
 103 silica beads (A) before and (B) after the AuNPs embedding. Similar to XPS, the EDS
 104 study showed the presence of gold after the AuNP embedding.



105

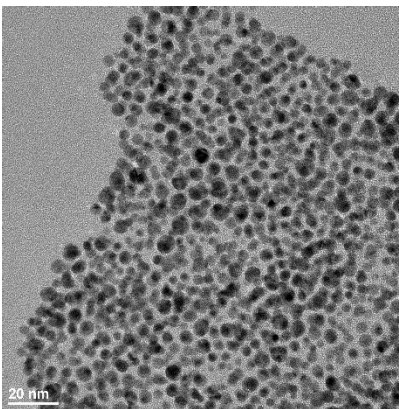
106 **Fig. S2.** UV-vis spectra of Au/SiO₂, porous SiO₂ and AuNPs. DMAP-AuNPs (red solid
 107 line); Porous silica beads before (black dash line) and after (black solid line) AuNPs

108 embedding. The resulting catalysts exhibited a similar UV-visible absorption (around 520
109 nm) as the original AuNPs.



110

111 **Fig. S3.** XPS survey scan of (A) Porous SiO₂ beads and (B) DMAP-AuNPs.



112

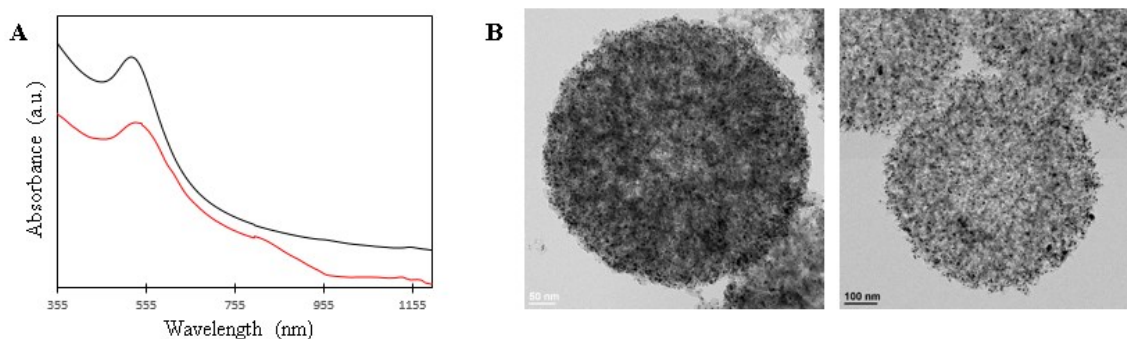
113 **Fig. S4.** TEM image of DMAP-AuNPs.

114

115 **Stability of Au/SiO₂**

116 The aqueous solution of the Au/SiO₂ catalyst (3 mg/ml) was placed in a water bath
117 sonication and was continuously sonicated for 17h.
118 The comparison was made between the UV-visible absorption spectra of Au/SiO₂ before
119 and after the sonication. It showed that there was negligible difference between the two
120 UV-visible absorption spectra. TEM images of Au/SiO₂ before and after the sonication
121 also showed there was no obvious difference. Both characterizations indicated that the
122 interaction between gold and silica was relatively strong; the Au/SiO₂ was a stable
123 catalyst.

124



125

126 **Fig. S5.** Stability test of the Au/SiO₂. A. UV-vis spectra of Au/SiO₂ before (black) and
127 after (red) 17 h sonication; B. TEM images of Au/SiO₂ before (left) and after (right) 17 h
128 sonication.; .

129

Table S1. Zeta potential of various samples

Sample Name	Zeta Potential/mV
DMAP-AuNPs	21.02
porous silica beads	-29.81
Au/SiO ₂	-19.25

130

131 **3. The weight percentage of Au in the Au/SiO₂ composite**

132 The weight percentage of Au in the Au/SiO₂ composite was determined by inductively
133 coupled plasma optical emission spectrometry (ICP-OES).

134 Sample preparation: 100 μL aqua regia (excess amount) was added to 500 μL of Au/SiO₂
135 catalyst solution with a known concentration of SiO₂ (the concentration of SiO₂ was

136 calculated from the original weight of SiO₂ beads dissolved in the water). After the gold
137 was completely dissolved, the solution was centrifuged, and the silica beads were
138 removed. 292 μL of the supernatant was added into 11.708 mL of 2% (weight percentage)
139 HNO₃.

140 Characterization details: ICP-OES analysis was performed on a Thermo Scientific ICAP
141 6000 series with Liquid Argon ICP-grade (Megs) as gas and RACID 86 Charge Injection
142 Device (CID) as the detector.

143

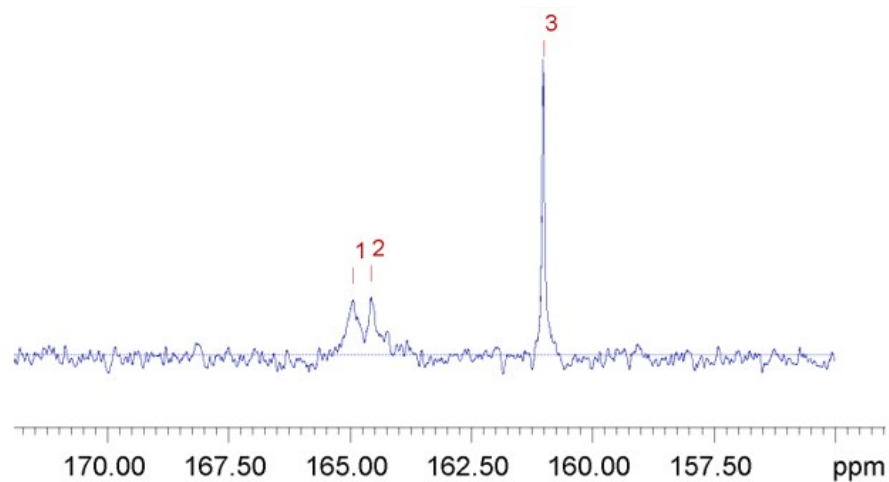
144 **4. Quantitative ¹³C NMR**

145 To establish a quantitative ¹³C NMR method, we took carbon relaxation time (T1) and
146 Nuclear Overhauser Enhancement (NoE) into our criteria. Unless special mention, all the
147 NMR samples for quantitative ¹³C NMR contained 400 μL D₂O, 300 μl PEHA CO₂
148 capture solution, and a known amount of imidazole (around 1 mmol). All the NMR
149 spectra were taken at 25 °C.

150 T1 measurements were done on a Bruker AVIIIHD 800 MHz NMR Spectrometer. An
151 NMR sample that contained 3.2 wt.% PEHA CO₂ capture solution was measured (Fig.
152 S6). The longest T1 is 16.5s, belonging to bicarbonates. Given that the delay time (D1)
153 should not be less than 5*T1 in order to obtain a quantitative ¹³C NMR, D1 was chosen to
154 be 85s. To eliminate NoE, two pulse sequences can be used: zg and zgig. The internal
155 standard imidazole was used as a compound to test if NoE is eliminated. Both pulse
156 sequences fit our needs.

157 The final quantitative ¹³C NMR method was chosen to have the following parameters:
158 Number of Scan=128; D1=85s; zgig (an inverse gated-decoupling pulse sequence).

159



Peak name	F2 [ppm]	lo	error	T1 [s]	error	a	error	fitInfo
1	164.502	1.02e+07	1.907e+06	11.7	7.630	1.14	0.1999	Done
2	164.110	9.79e+06	1.810e+06	5.86	3.458	1.41	0.2798	Done
3	160.335	5.82e+07	1.505e+06	16.5	1.268	1.39	0.03198	Done

160

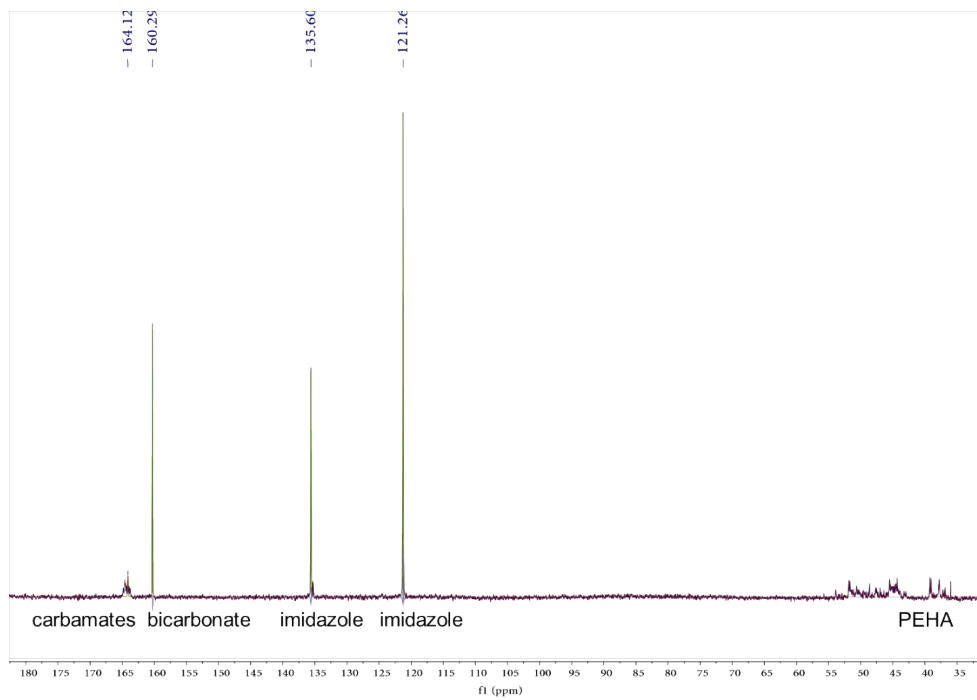
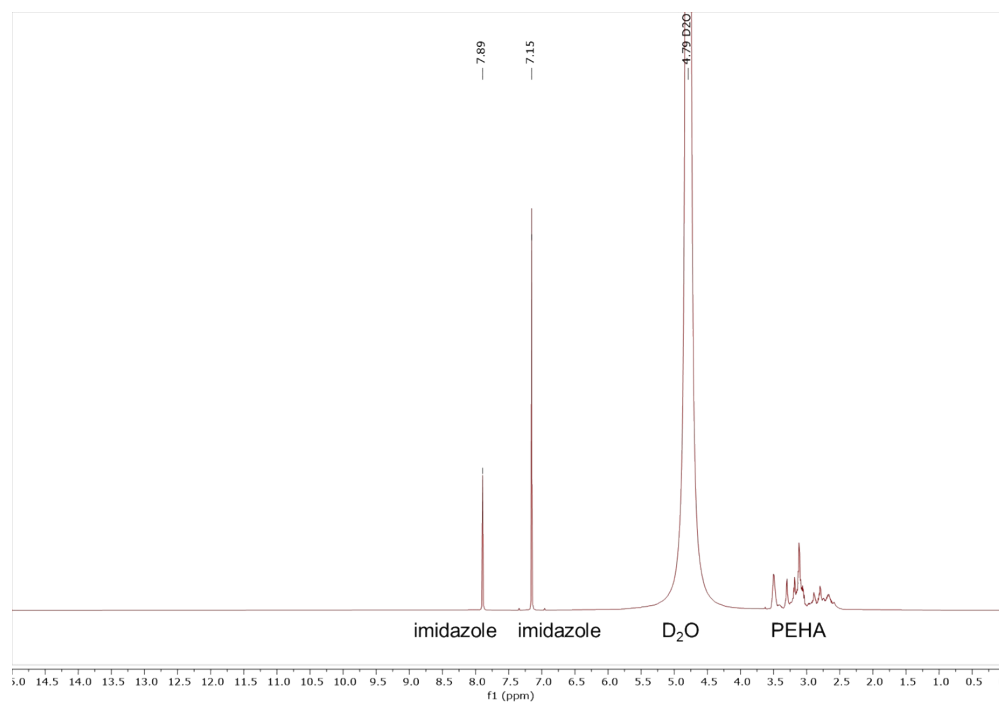
161 **Fig. S6.** ^{13}C NMR and T1 measurements of carbamates and bicarbonates in 3.2 wt.%

162 PEHA CO_2 capture solution. Peak 1 and 2 are the signals of carbamates, and Peak 3 is the

163 signal of bicarbonates.

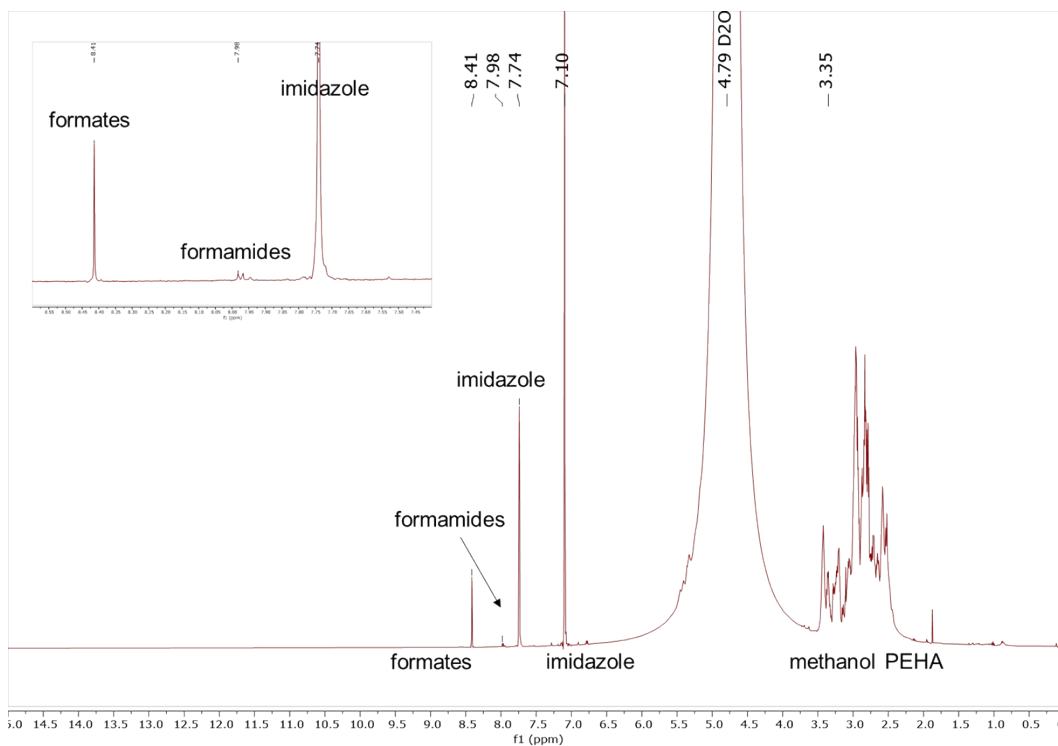
164

165

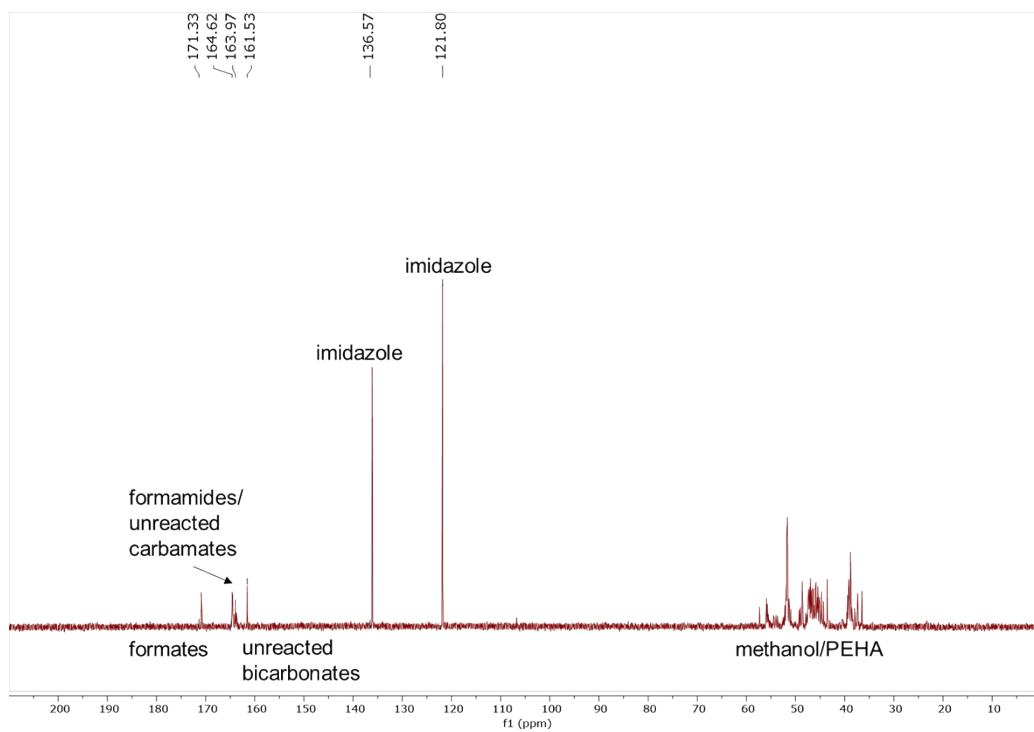


168 **Fig. S7.** NMR spectra of 3.2 wt. % PEHA CO₂ capture solution (imidazole as an internal
169 standard). Above: ¹H NMR. Below: quantitative ¹³C NMR.

170



171



172

173 **Fig. S8.** NMR spectra of 3.2 wt. % PEHA CO₂ capture solution after hydrogenation
 174 (imidazole as an internal standard). Above: ¹H NMR. Below: non-quantitative ¹³C NMR.

175

176 **5. GC-TCD analysis of gas phase**

177 Gas phase after the hydrogenation was collected by a Tedlar® gas sampling bag.
178 Specifically, the outlet of the Biotage® Endeavor™ Catalyst Screening System and a
179 vacuum pump were connected to the gas sampling bag via a 3-way line connector valve.
180 Firstly, the gas sampling bag and all the linings were vacuumed; secondly, the gas inside
181 the high-pressure reactor was released into and gathered by the gas sampling bag; excess
182 gas was evacuated as soon as the gas sampling bag was full by switching the 3-way valve.
183

184 Blank (no gas injection), 1 ml of the gas phase after hydrogenation, and 0.5 ml of various
185 gas standards (lab air, CO₂, H₂, CO, CH₄, O₂, N₂) were analyzed by GC-TCD
186 respectively. Each sample was repeated at least twice.

187 Table S2 shows the retention time of gas standards, as well as to-be-determined peaks
188 presented in the gas phase after the hydrogenation. Fig. S9 shows the GC-TCD of the gas
189 phase after the hydrogenation. CO₂, O₂, N₂ were from air trapped in the needle of the gas
190 sampler syringe. H₂ was one of the reactants. CO was not detectable using this instrument
191 and sampling method. Based on the limit of detection (LOD) and limit of analysis (LOA)
192 (Section 6 Table S3), we conclude that the CO in the gas phase after the hydrogenation, if
193 assuming it existed, should be below 0.05 ml.

194 ***Table S2. Retention time of various samples in GC-TCD***

A. Gas standards*

Component	CO₂	Noise	H₂	O₂	N₂	Noise	CH₄	CO
Retention Time/min	6.2	9.1	13.3	14.2	14.9	15.6	16.2	17.1

B. Gas phase after hydrogenation**

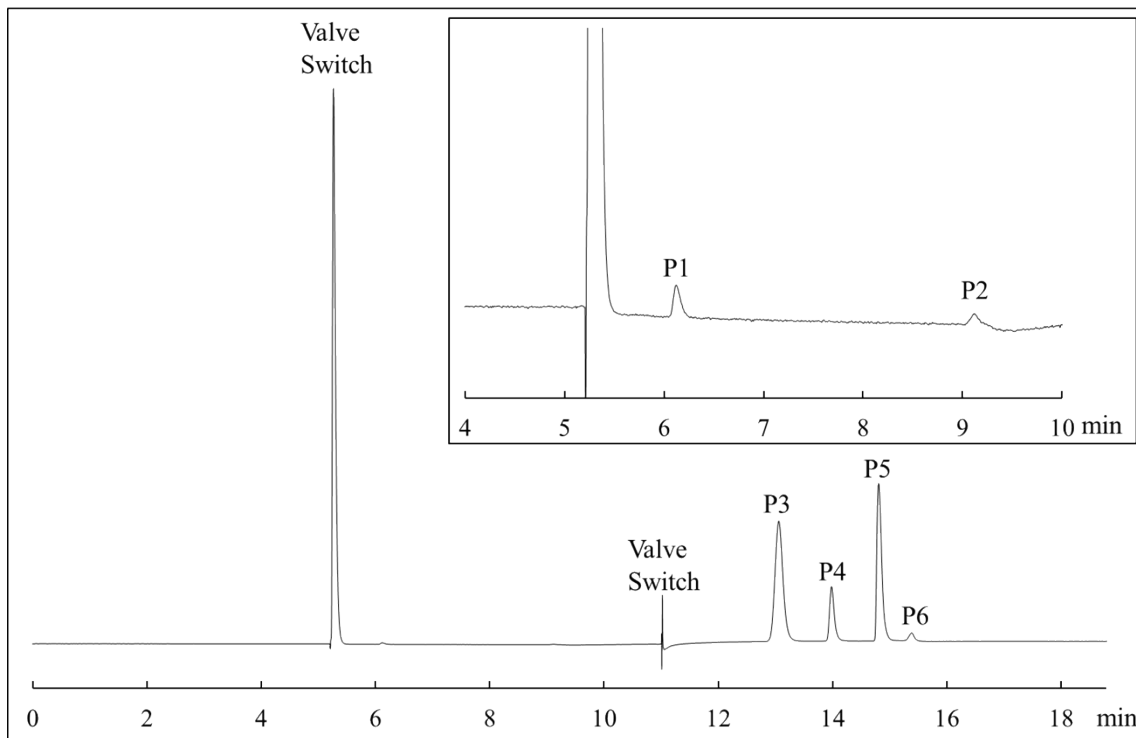
Component	P1	P2	P3	P4	P5	P6
Retention Time/min	6.1	9.1	13.0	14.0	14.8	15.4

195

196 *The two noises are attributed to leaks in the injector and valve switch, appearing
197 whenever an injection happens.

198 **Reaction condition: 600 μL 3.2 wt. % PEHA CO₂ capture solution, 1 mL H₂O
199 containing 5.29 mg Au/SiO₂ and boric acid (1 mol % corresponding to the amount of

200 PEHA presented in the CO₂ capture solution), and 16 bar H₂ (25 °C). The entire system
201 was stirred at 500 rpm, 100 °C for 36 hours.



202

203 **Fig. S9.** GC-TCD of the gas phase after a typical hydrogenation reaction. The insert
204 chromatograph is the zoom-in section of retention time= 4-10 min. According to *Table*
205 *S2*, P1-P6 are identified to be CO₂, noise, H₂, O₂, N₂, and noise.

206

207 **6. Limit of detection (LOD) and limit of analysis (LOA) determination on GC-TCD**

208 In order to determine the LOD and the LOA, the GC was “injected” with a “blank
209 sample” ten times.

210 The blank was the run initiated without a volume of gas introduced. The peak height was
211 measured at the base corresponding to a gas analyte. The mean and standard deviation
212 was determined. The LOD was three times the standard deviation at the point where the
213 analyte peak should have occurred. The LOA was ten times the limit of detection. The
214 signal was validated by the injection of a pure gas sample at the limit of detection.

215 Two gases, nitrogen and oxygen were excluded because of a constant leak from the
216 switch valve.

217 The gas standard used in calibration is a certificated gas mixture purchased from Praxair
 218 Canada Inc. The gas components and their molar concentrations can be found in Fig. S10.

219 **Table S3. Limits of detection (LOD) and limits of analysis (LOA) (ml) of gas**

Gas	LOD (ml)	LOA (ml)
CO ₂	0.005	0.01
H ₂	0.005	0.01
CO	0.05	0.1

220 **standard**

CERTIFICATE OF ANALYSIS
Certified Standard

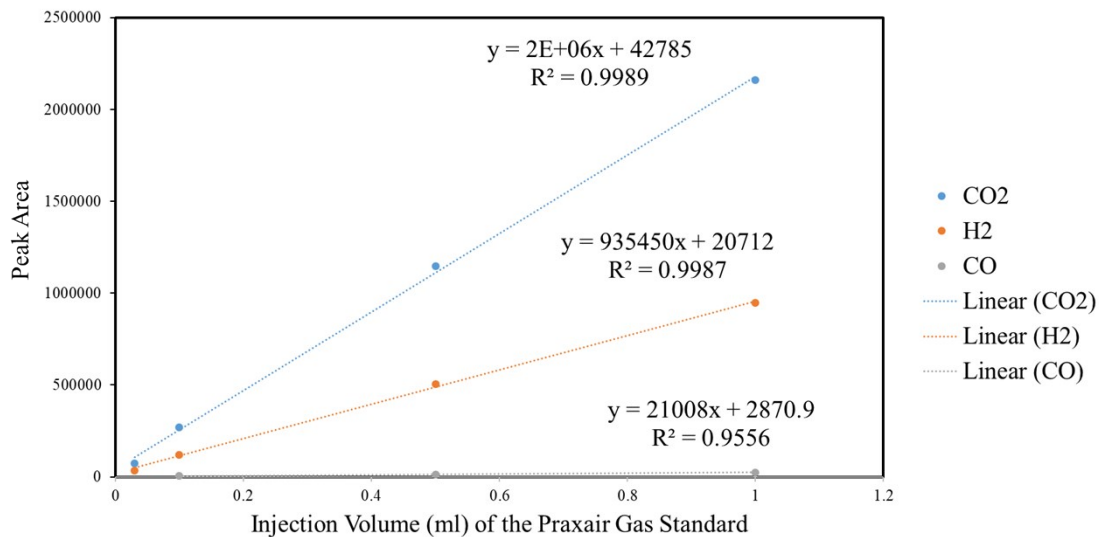
Component	Requested Concentration (Molar)	Certified Concentration (Molar)	Analytical Reference	Analytical Uncertainty
Ethylene	5 %	5.04 %	1	± 0.10%
Methane	1 %	1.00 %	1	± 0.02%
Carbon monoxide	1 %	1.01 %	1	± 0.02%
Hydrogen	5 %	5.04 %	1	± 0.10%
Carbon dioxide	Balance	Balance		

Cylinder Style: **A3** Fill Date: **8/17/2020** Filling Method: **Transfill**
 Cylinder Pressure @ 70°F: **659.64 psig** Analysis Date: **8/18/2020**
 Cylinder Volume: **.36 M3**
 Valve Outlet Connection: **CGA 350**
 Cylinder Number(s): **EA0017694**

Comments: **The analytical data and all QC contained in this Certificate of Analysis was reviewed and accepted by the following individual(s):**

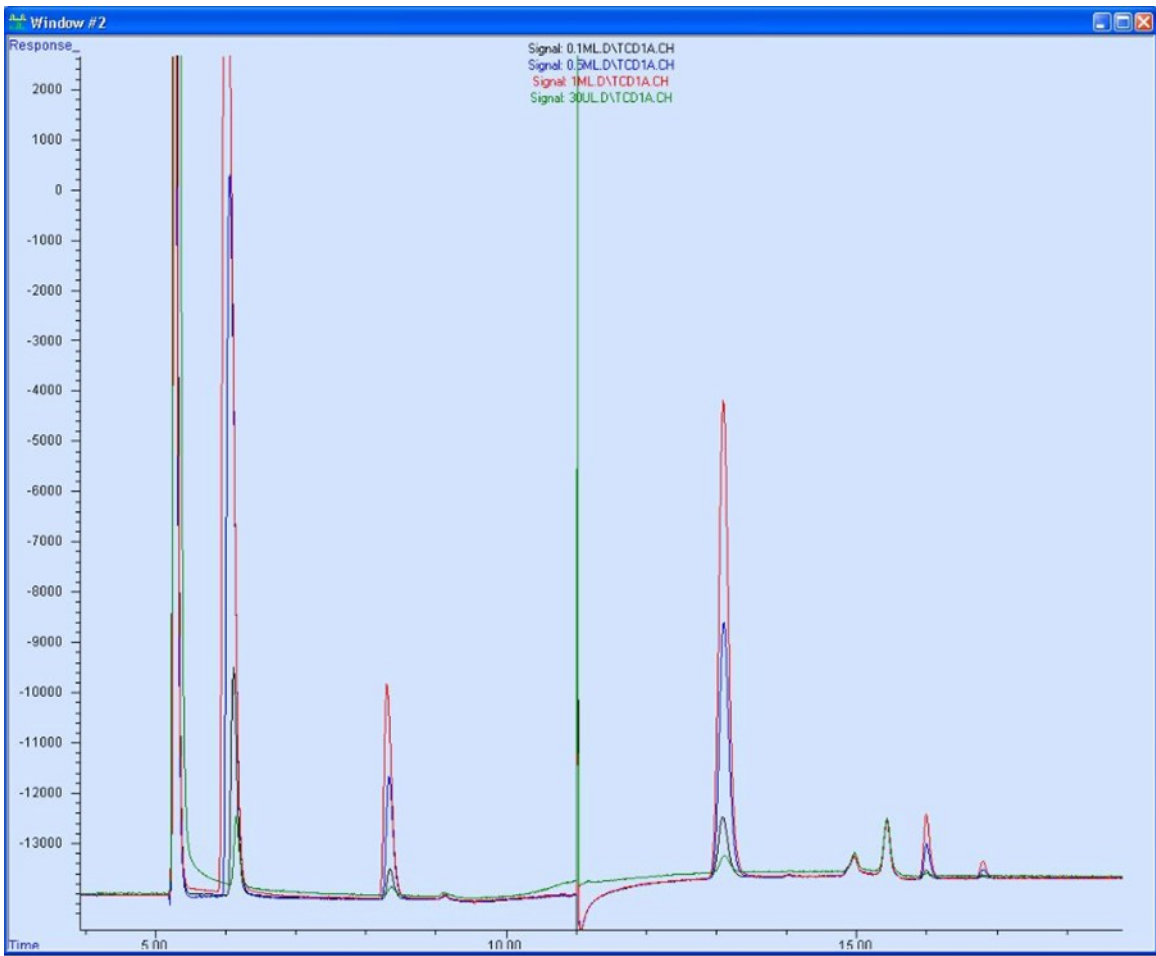
221

222 **Fig. S10.** Certificate of the gas standard used in the calibration curves and the
 223 determination of LOD and LOA.

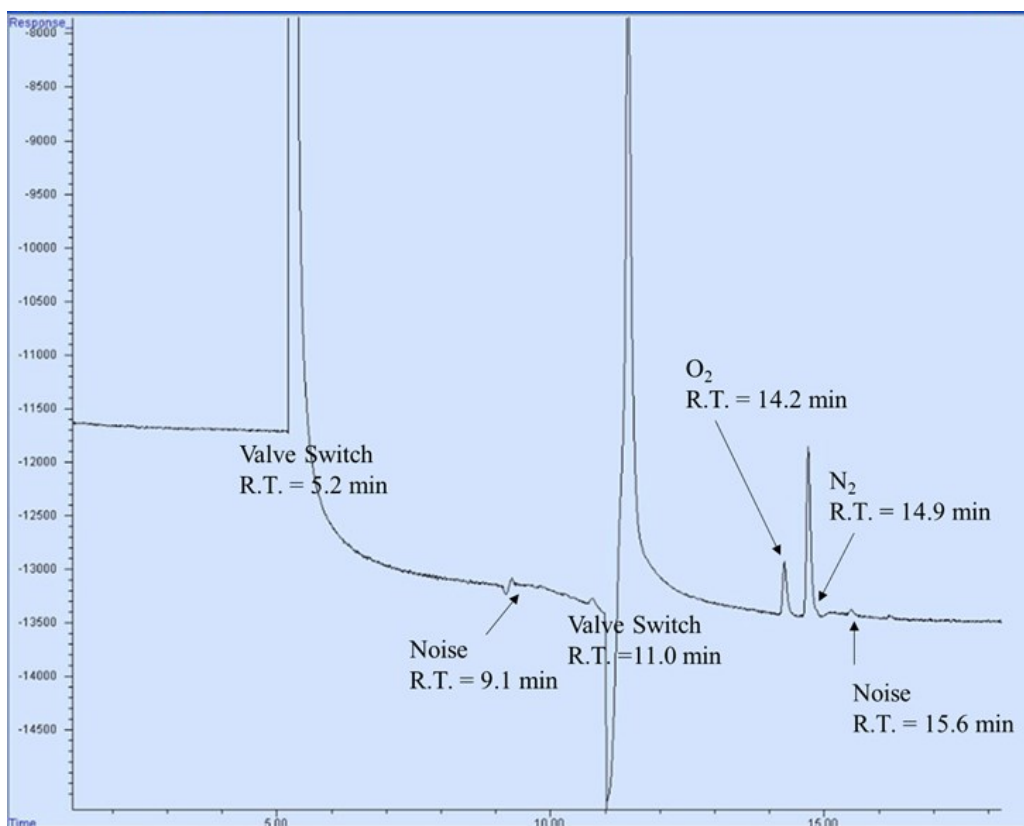


224 **Fig. S11.** Calibration curves. The injection volumes (ml) of the Praxair gas standard were
 225 0.03, 0.1, 0.5, and 1.

226



227 **Fig. S12.** Gas chromatographs of the gas standard with various injection volumes.



229

230 **Fig. S13.** Gas chromatographs of the blank (no gas injection).

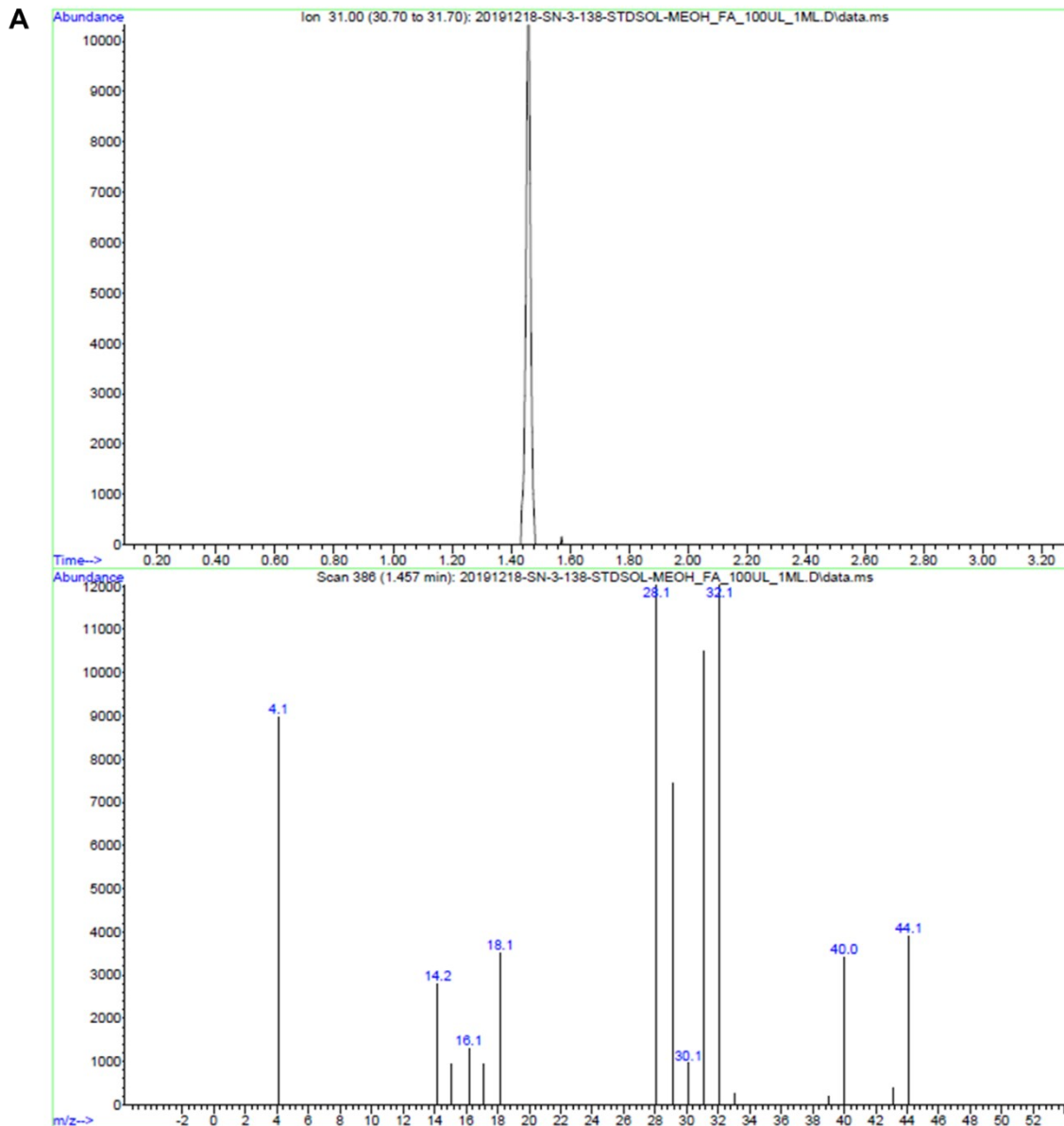
231

232 **7. GC-MS identification and quantification of MeOH**

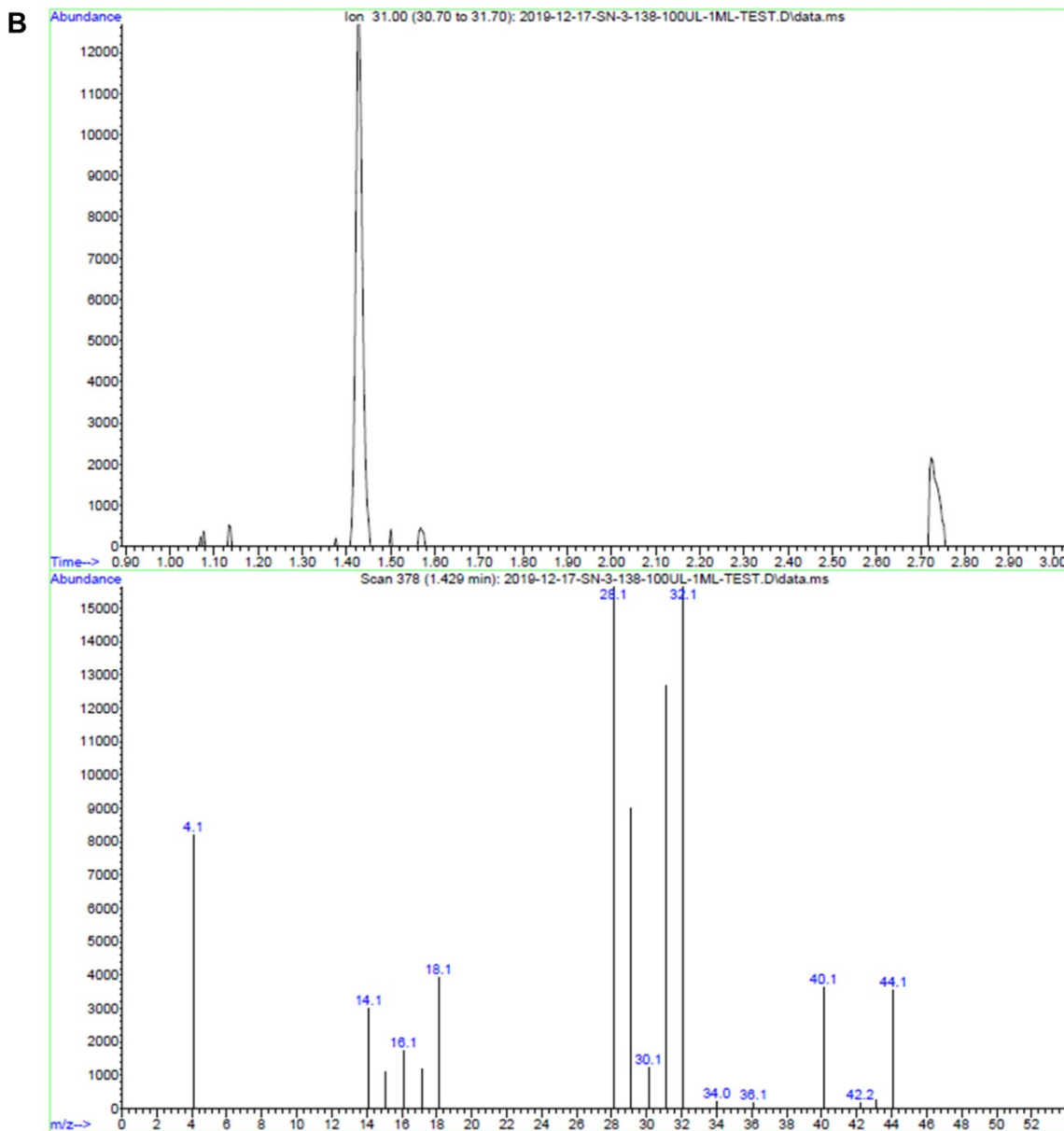
233 The signal of MeOH is within the regions of PEHA -CH₂- in ¹H NMR. Sometimes, due
 234 to low MeOH concentrations in reaction mixtures, it was difficult to quantify the yield of
 235 MeOH depending on ¹H NMR. Thus, an additional step of GC-MS characterization was
 236 used to identify and quantify the MeOH in the hydrogenated products.

237 The large quantities of salts (formate and unreacted bicarbonates) presented in the
 238 product mixture made a direct injection of our liquid sample into a GC-MS unlikely. An
 239 alternative sample injection method was thus developed. 100 μL sample was injected into
 240 a pre-vacuumed chamber, resulting in the evaporation of volatile chemicals (like MeOH)
 241 but not the salts. 1 mL gas sample was then taken from the chamber and injected into
 242 GC-MS.

243 Compared to a standard aqueous solution containing MeOH, the reaction mixture had a
244 similar peak with identical retention time and MS spectrum (Fig. S14). These are
245 consistent with the presence of MeOH in the hydrogenation products.



246



247

248 **Fig. S14.** GC-MS.

249 A. A standard aqueous solution containing MeOH and formic acid.

250 B. A reaction mixture after hydrogenation.

251 Both samples were treated with the same sample preparation/injection method. MeOH
 252 has a retention time of 1.4 min in both A and B. The fragments from air were visible in
 253 both MS spectra of A and B, because the dead volume in the gas sampler syringe made
 254 air being also injected into the GC-MS.

255

256 **8. Mechanistic studies:¹⁸O isotope study**

257 To further understand the role of Pathways I and II in the generation of methanol,
258 formamide was hydrogenated in H₂¹⁸O. After the reaction, a portion of the reaction
259 mixture was analyzed by ¹H NMR with imidazole as an internal standard, to obtain the
260 total quantity of methanol present. Another portion of the reaction mixture was analyzed
261 by the procedure described in the previous section, *GC-MS identification and*
262 *quantification of MeOH*, to identify Me¹⁸OH and quantify Me¹⁶OH (Fig. S15, B).

263 A methanol (Me¹⁶OH) standard solution in GC-MS establishes that methanol has a
264 retention time of 1.205 min under the experimental conditions. This retention time was
265 less than the one shown in Fig. S14, because approximately 1 m of the column was
266 removed (cut) between these two experiments. This removal was necessitated by
267 maintenance of the GC-MS. Fig. S15, B demonstrates the presence of Me¹⁸OH and
268 Me¹⁶OH, with the former being dominant. It is notable that m/z=33.1 and m/z=34.1 occur
269 naturally (Fig. S15 A), but with low abundances. Given the dramatic contrast between
270 Fig. S15, A and B in terms of the abundances of these two ion fragments, we are
271 confident in assigning the two ion fragments in B to Me¹⁸OH. A new ion fragment
272 m/z=35.1 further establishes the existence of Me¹⁸OH.

273 *Semi-quantification methodology explanation*

274 One of the standard methods to quantify a chemical of interest is to build a calibration
275 curve on the peak area of a primary ion fragment in ion fragment chromatogram, for
276 example, m/z=29 or 31 in the case of methanol. (*J. Chromatogr. A 1017 (2003) 151–159*)

277 Nevertheless, this approach is not applicable in our case. On the one hand, the peak area
278 of the m/z=31 in the ion fragment chromatogram of Fig. S15, B corresponds to two
279 species: Me¹⁸OH and Me¹⁶OH. On the other hand, the peak area of m/z=29 is not usable
280 either, given the primary interference from N₂ and the minor interference from formic
281 acid. Although only 0.74% compared to the m/z=28 in the relative abundance (NIST
282 Standard Reference Database 69: *NIST Chemistry WebBook*), the m/z=29 from N₂ arises
283 as primary background noise in our case. Use of a methodology based on peak areas in an

284 ion fragment chromatogram to analyze Fig. S15, B will result in a peak area of $m/z=29$
285 consisting of N_2 , $Me^{16}OH$, and formic acid.

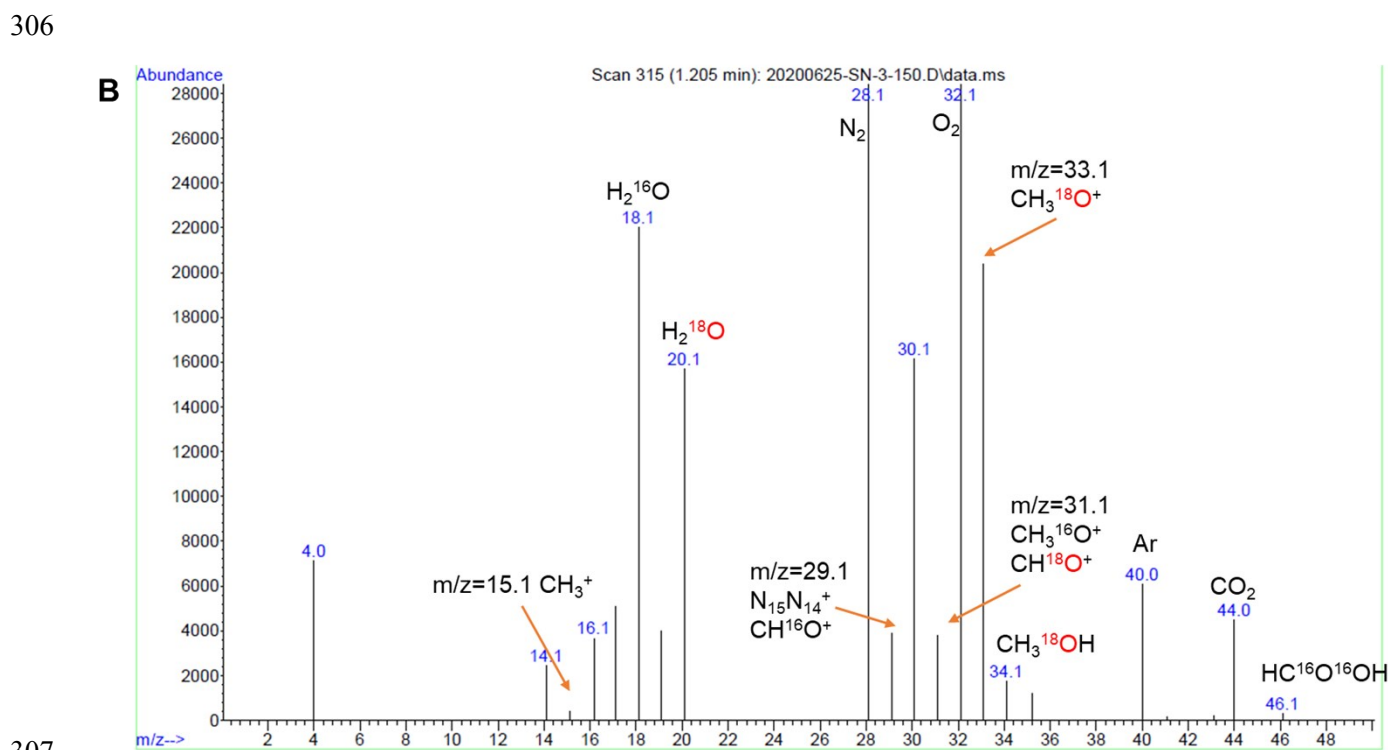
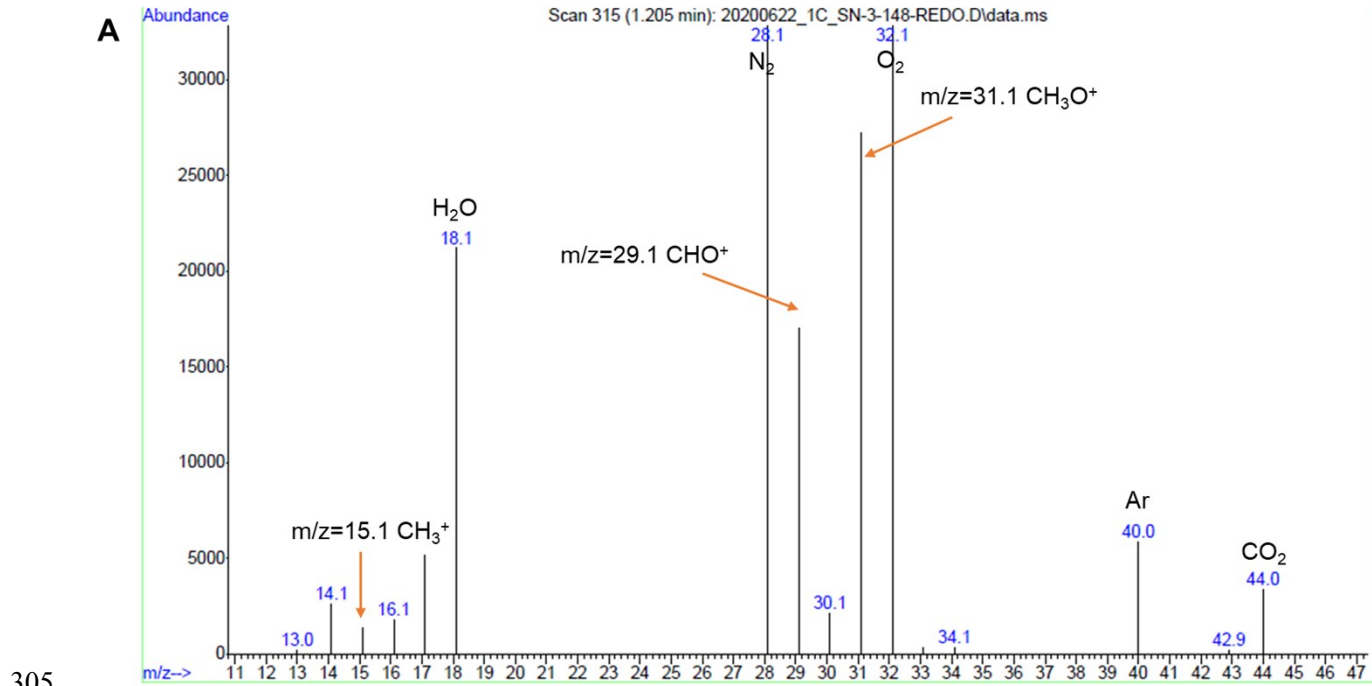
286 Considering the above, we decided to quantify $Me^{16}OH$ based on the abundance of the
287 $m/z=29$ in mass spectra at 1.205 min, the retention time of methanol. Similar methods are
288 used in label-free quantitative proteomics (*Current Genomics*, 2008, 9, 263-274). The
289 limited accuracy of this methodology is sufficient for this semi-quantification purpose,
290 because this study is interested in which category the ratio of $Me^{18}OH$ to $Me^{16}OH$ falls
291 into: 0, between 0 and 1, or ≥ 1 . The credibility of this method is based on:

- 292 a) the negligible presence of formic acid at 1.205 min;
- 293 b) the nearly identical retention time of $Me^{18}OH$ and $Me^{16}OH$;
- 294 c) the ability to quantify the exact N_2 contribution to $m/z=29$ at 1.205 min via running a
295 blank solution;
- 296 d) the assumption that the chromatography peaks of $Me^{18}OH$ and $Me^{16}OH$ are
297 symmetrical with nearly identical half peak widths.

298 *Calibration curve and calculation of the ratio of $Me^{18}OH$ to $Me^{16}OH$*

299 In order to mimic the product distribution in typical CO_2 hydrogenation catalyzed by our
300 $Au(0)$ catalyst, we prepared the stock solution by adding 6 μL formic acid (88%) and 6
301 μL methanol to 6 mL water. We diluted this stock solution into standard solutions, while
302 the blank was water. The calibration curve and original data are shown in Fig. S16.
303 Finally, we determined the mole ratio of $Me^{18}OH$ to $Me^{16}OH$ to be 3.5:1.

304



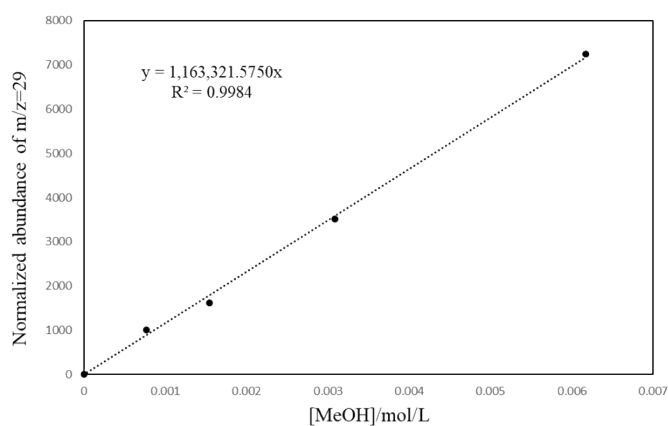
308 **Fig. S15.** Mass spectra.
 309 A. A standard solution containing Me¹⁶OH and formic acid.
 310 B. The reaction mixture after formamide hydrogenation in H₂¹⁸O. It is worth noticing that
 311 the normalized abundance (after subtracting the N₂ background) of m/z=29 is 2127, about

312 half in the abundance of $m/z=31$, which is in agreement with a typical MS pattern of
313 Me^{16}OH where $m/z=31$ is higher than $m/z=29$.

314

A	[MeOH]/mol/L	Abundance of $m/z=29$	Normalized abundance of $m/z=29$
	0.00617	9011	7242
	0.00308	5289	3520
	0.00154	3388	1619
	0.000771	2778	1009
	0	*1769	0
	Formamide hydrogenation in ^{18}O -water	3896	2127

B



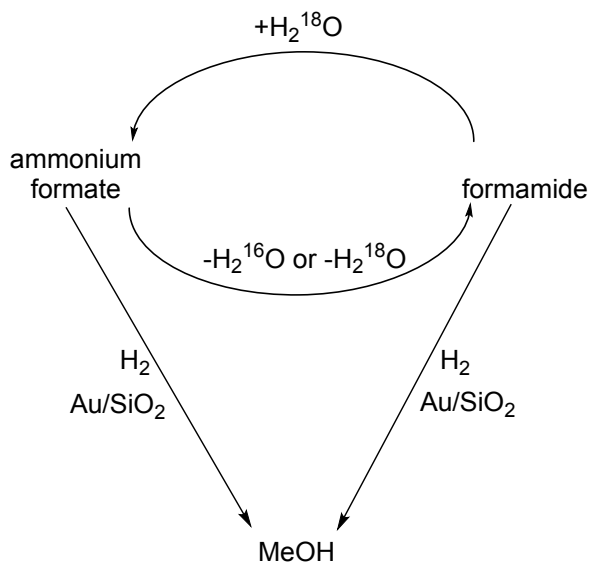
315

316 **Fig. S16.** Calibration curve.

317 A. Raw data showing the abundance of $m/z=29$ at retention time=1.205 min. *The
318 $m/z=29$ signal in the blank is from $M+1$ of N_2 , constant background as the amount of N_2
319 presented in all the samples should be identical, given that the same sample preparation
320 method, injection method, and injection syringe were used every time.

321 B. Calibration curve.

322



323

324 **Fig. S17.** Potential transformations in the isotopic studies.

325

326 **9. Additional studies**

327 **Table S4.** Recently reported systems of amine-captured CO₂ hydrogenation to C1

328 products in (partially) aqueous conditions similar to this work

Catalyst	Temp/°C	Base	Solvent	P(H ₂ /CO ₂)/bar	Time/h	Products	Conversion/%	No. of cycles before catalysts lost 20% activity	Ambient air as CO ₂ source: studied	Ref.
AuNP/SiO ₂	100	PEHA	H ₂ O	16/3	48	formate, formamide, MeOH	80	> 4	Yes	This work
AuNC ^a /SiO ₂ -Schiff	90	NEt ₃	H ₂ O/MeOH (v:v=1:4)	50/30	12	formate	- ^b	1	No	¹
Au/TiO ₂	40	NEt ₃	Neat	90/90	72	formate, CO	29	> 12	No	²
Ru-MACHO-BH	145	PEHA	H ₂ O/2M-THF (v:v=3:5)	80/1	72	formate, formamide, MeOH	95	>4	Yes	³

329 a. AuNC stands for gold nanoclusters (d = ~1.5 nm). b. The yield or the conversion was
330 not given.

331

332 Reference:

333 1. Q. Liu, X. Yang, L. Li, S. Miao, Y. Li, Y. Li, X. Wang, Y. Huang and T. Zhang,
334 *Nature Communications*, 2017, **8**, 1407.

- 335 2. D. Preti, C. Resta, S. Squarcialupi and G. Fachinetti, *Angewandte Chemie*
 336 *International Edition*, 2011, **50**, 12551-12554.
 337 3. S. Kar, R. Sen, A. Goeppert and G. K. S. Prakash, *Journal of the American*
 338 *Chemical Society*, 2018, **140**, 1580-1583.

339

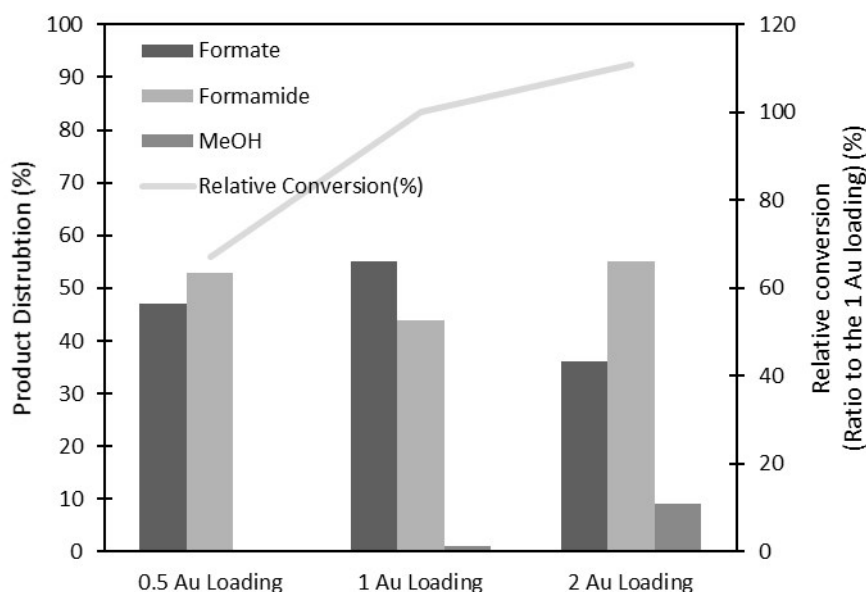
340 **Table S5.** Study of CO₂ hydrogenation in dilute PEHA solutions

Entry	wt % of PEHA in water	CO ₂ capture			Hydrogenation ^b			Conversion(%) ^c
		Mole ratio of carbamate: bicarbonate ^a	CO ₂ capacity ^a (mmol of CO ₂ /(g of PEHA))	CO ₂ capacity ^a (mmol of CO ₂ /(ml of capture solution))	Product distribution			
					Formate (%) ^c	Formamide (%) ^c	MeOH (%) ^c	
1	3.2	1:1	14.45	0.49	55	44	1	68
2	1.6	1:2	8.06	0.26	38	54	8	16
3	0.8	1:5	12.54	0.10	24	54	22	40

341

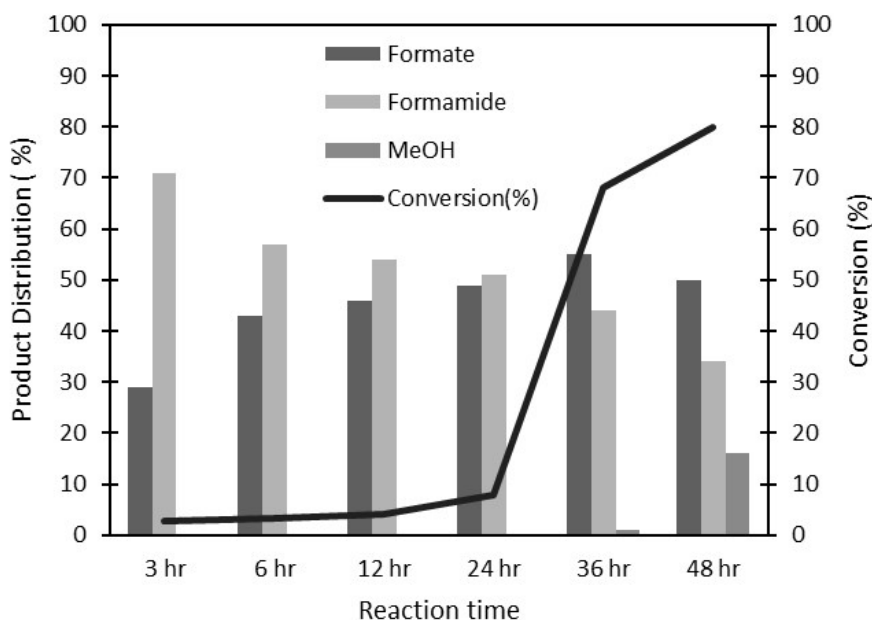
342 Notes: a. The CO₂ capacity, identification and quantification of carbamate and
 343 bicarbonate were determined by quantitative ¹³C NMR with imidazole as an internal
 344 standard. b. Hydrogenation reaction conditions: 600 μL CO₂ capture solution, 1 mL H₂O
 345 containing 5.29 mg Au/SiO₂ and boric acid (1 mol % corresponding to the amount of
 346 PEHA presented in the CO₂ capture solution), and 16 bar H₂ (25 °C). The entire system
 347 was stirred at 500 rpm, 100 °C for 36 hours. c. The selectivity and overall conversion
 348 were based on ¹H NMR with imidazole as an internal standard.

349



350

351 **Fig. S18.** Catalytic activities with different Au loadings. 1 Au loading meant 5.29 mg
 352 Au/SiO₂; 2 Au loading meant 10.58 mg Au/SiO₂, etc. Reaction conditions: 600 μL 3.2 wt. %
 353 PEHA CO₂ capture solution, 1 mL H₂O containing Au/SiO₂ and boric acid(1 mol %
 354 corresponding to the amount of PEHA presented in the CO₂ capture solution), and 16 bar
 355 H₂ (25 °C). The entire system was stirred at 500 rpm, 100 °C for 36 hours.
 356



357

358 **Fig. S19.** Product distribution and conversion with various reaction times. Reaction
 359 conditions: 600 μL 3.2 wt. % PEHA CO₂ capture solution, 1 mL H₂O containing 5.29 mg
 360 Au/SiO₂ and boric acid(1 mol % corresponding to the amount of PEHA presented in the
 361 CO₂ capture solution), and 16 bar H₂ (25 °C). The entire system was stirred at 500 rpm,
 362 100 °C.